AAC
Journals.ASM.org

Population Pharmacokinetics of Palivizumab, a Humanized Anti-Respiratory Syncytial Virus Monoclonal Antibody, in Adults and Children

Gabriel J. Robbie,[a] Liang Zhao,[a]* John Mondick,[b] Genevieve Losonsky,[a] and Lorin K. Roskos[a]

MedImmune, Gaithersburg, Maryland, USA,[a] and Metrum Research Group, Tariffville, Connecticut, USA[b]

Although it has been on the market for over a decade, confusion remains regarding the pharmacokinetics (PK) and optimal dosing of palivizumab, a humanized IgG1κ monoclonal antibody indicated for the prevention of serious lower respiratory tract disease caused by respiratory syncytial virus (RSV) in pediatric patients at high risk of RSV disease. The objectives of this analysis were to characterize the population PK of palivizumab in adults and children using nonlinear mixed-effect modeling, quantify the effects of individual covariates on variability in palivizumab disposition, and compare palivizumab exposures for various dosing scenarios. Palivizumab PK data from 22 clinical studies were used for model development. The model was developed using a two-stage approach: (i) a 2-compartment model with first-order absorption after intramuscular administration was fitted to adult data, and (ii) the same structural model was fitted to the sparse pediatric data using the NONMEM $PRIOR subroutine, with informative priors obtained from the adult analysis. Body weight and an age descriptor that combines gestational age and postnatal age (PAGE) using an asymptotic-exponential model best described palivizumab clearance in pediatric patients. Palivizumab clearance increased slightly from 10.2 ml/day to 11.9 ml/day as a function of PAGE ranging from 7 to 18 months. Covariate analysis indicated a 20% higher clearance in children with chronic lung disease and in children with antidrug antibody titer values of ≥80. These covariates did not substantially explain interindividual variability. In the label-indicated pediatric population, body weight was the primary demographic factor affecting palivizumab PK. Body weight-based dosing of 15 mg/kg yields similar palivizumab concentrations in children of different gestational and postnatal ages. Simulations demonstrated that there was little difference in palivizumab PK between healthy term and premature infants. Simulations also demonstrated that the 5 monthly palivizumab doses of 15 mg/kg, consistent with the label and studied in two randomized, clinical trials, provided greater and more prolonged palivizumab exposure than did an abbreviated dosing regimen of 3 monthly doses.

Respiratory syncytial virus (RSV) is a respiratory pathogen of infants and young children that causes annual epidemics of bronchiolitis and pneumonia worldwide (6, 14). The peak incidence of severe RSV disease occurs between 2 and 3 months of age, and the main risk factors include prematurity, chronic lung disease (CLD; formerly known as bronchopulmonary dysplasia), and congenital heart disease (24, 25, 27). RSV is estimated to cause as much as 75% of all childhood bronchiolitis and up to 40% of all pediatric pneumonias (15). Lower respiratory tract disease due to RSV accounts for more than 125,000 pediatric hospitalizations and approximately 6.3 deaths per 100,000 person-years among children <4 years of age in the United States. Despite improvements in treatment, there is a 3% to 4% case fatality rate in infants with heart and/or lung disease who are hospitalized with RSV infection, whereas the overall infant case fatality rate due to RSV disease has been documented as 1% (27).

Palivizumab is a humanized monoclonal antibody produced by recombinant DNA technology, directed to an epitope in the A antigenic site of the F protein of RSV. Palivizumab provides neutralizing and fusion-inhibitory activity against RSV, resulting in inhibition of RSV replication.

Palivizumab has been studied extensively in premature children and has demonstrated safety and efficacy at a dose of 15 mg/kg of body weight administered monthly for a total of 5 doses. The IMpact study enrolled 1,502 children who were of ≤35 weeks' gestational age (wGA) and ≤6 months of age, or ≤24 months of age with CLD. Prophylaxis with palivizumab reduced the incidence of RSV-associated hospitalizations by 55% compared with placebo (17). Based on these data, palivizumab was licensed in 1998 by the U.S. Food and Drug Administration for the prevention of serious lower respiratory tract disease caused by RSV in pediatric patients at high risk of RSV disease. The Palivizumab Outcomes Registry, a nationwide registry of 2,116 high-risk children who received palivizumab after U.S. Food and Drug Administration approval, demonstrated hospitalization rates of 2.9% for pediatric patients at high risk for RSV disease who were administered palivizumab prophylaxis compared with the 4.8% reported in the IMpact study (22).

Only trough serum concentrations were collected in the pivotal pediatric clinical efficacy study (MI-CP018; IMpact) (17); therefore, the pharmacokinetics (PK) of palivizumab is mainly described in the literature as mean trough concentrations and half-lives that range from 17 days (23) to 26.8 days (26). These trough concentrations listed in the palivizumab package insert

Received 29 December 2011 Returned for modification 1 February 2012
Accepted 25 June 2012
Published ahead of print 16 July 2012
Address correspondence to Gabriel J. Robbie, robbieg@medimmune.com.
* Present address: Liang Zhao, U.S. Food and Drug Administration, Silver Spring, Maryland, USA.

doi:10.1128/AAC.06446-11
The authors have paid a fee to allow immediate free access to this article.

TABLE 1 Clinical trials used in pharmacokinetic modeling[a]

Study	Subject population	Route of administration, dose (mg/kg) of palivizumab	No. of subjects	PK sampling schedule
MI-CP004	Adult transplant recipients	i.v., 15	6	Days 0 to 45
MI-CP005	Preterm infants and children with BPD aged <24 mo	i.v., 3, 10, 15	42	Hour 1 and days 0, 2, 15, 30, 32, 45, 60, 90, 120, and 150
MI-CP007	Healthy adults	i.m., 3	4	Hours 0.25, 0.5, 1, 4, 8, 12, and 24 and days 2 to 5, 7, 14, 21, 32, 33, 24, 35, 37, 44, 51, and 60
MI-CP009	Hospitalized children with RSV aged ≤24 mo	i.v., 5, 15	59	Days 0 to 30
MI-CP011	Preterm infants and children with BPD aged ≤24 mo	i.m., 5, 10, 15	65	Days 2, 7, 14, 30, 32, 37, 44, 60, 90, 120, and 150
MI-CP012	Preterm infants and children with BPD aged ≤24 mo	i.m., 5, 15	59	Days 7, 30, 60, 90, 120, and 150 and days 2, 7, 14, 30, 32, 37, 44, 60, 90, 120, and 150
MI-CP013	Hospitalized children with RSV aged ≤24 mo	i.v., 5, 15	7	Days 0 to 30
MI-CP017	Healthy adults	i.v., 15	6	Hours 1, 4, 8, and 24 and days 2, 7, 14, and 60
MI-CP018	Preterm infants and children with BPD aged ≤24 mo	i.m., 15	1,002	Days 30, 60, 90, and 120
MI-CP026	Intubated infants with RSV	i.v., 15	35	Days 1, 2, and 30
MI-CP034	Adult transplant recipients	i.v., 15	15	EOI and days 7, 14, 21, and 28
MI-CP035	Healthy adults	i.v., 15, 30	12	Hours 1 and 24 and days 2, 7, 14, 21, 30, 45, and 60
MI-CP036	Preterm infants and children with BPD aged ≤24 mo	i.m., 15	55	Days 30 and 120
MI-CP045	Preterm infants and children with BPD aged ≤24 mo	i.v., 15, 30	21	Hour 1 and day 30
MI-CP080	Healthy adults	i.m., 3; i.v., 15	48	Days 1 to 5, 7, 14, 21, 30, 37, and 60
MI-CP097	Preterm infants	i.m., 15	153	Days 30 and 60
MI-CP9401a	Healthy adults	i.v., 3, 10, 15	12	Minutes, hours, and days[b]
MI-CP9401b	Healthy adults	i.v., 3, 10, 15	12	Minutes, hours, and days[b]
MI-CP9401c	Healthy adults	i.v., 3, 10, 15; i.m., 15	12	Minutes, hours, and days[b]
MI-CP116	Preterm infants and children with BPD aged ≤24 mo	i.m., 15	116	Day 120
MI-CP118	Preterm infants and children with BPD aged ≤24 mo	i.m., 15	70	Days 30 and 120
MI-CP127	Preterm infants and children with BPD aged ≤24 mo	i.m., 15	72	Days 60 and 150
Total			1,883	

[a] Samples were collected before dosing for all patients. Abbreviations: BPD, bronchopulmonary dysplasia; EOI, end of infusion; RSV, respiratory syncytial virus; i.m., intramuscular; i.v., intravenous; PK, pharmacokinetics.
[b] In studies MI-CP9401a, -b, and -c, blood was collected for PK analyses before dosing; at the end of infusion; at 5, 10, 15, and 30 min; at 1, 2, 4, 8, 12, and 24 h; and on days 2, 3, 7, 14, 21, 28, 35, 42, 49, and 56.

exhibit substantial interindividual variability. Measured 30 days after the first, second, third, and fourth intramuscular (i.m.) doses of palivizumab at 15 mg/kg, trough serum concentrations varied widely around the mean value: 37 ± 21, 57 ± 41, 68 ± 51, and 72 ± 50 μg/ml, respectively (19). This observation of interindividual variability in serum concentrations and the lack of adequate PK characterization of palivizumab highlighted the importance of developing a population PK model to describe the PK and identify factors that could help explain variability in serum concentrations. The specific objectives of this study were to develop a population PK model to describe the PK of palivizumab in adults and children and to evaluate the contribution of patient-specific demographic covariates and antidrug antibody (ADA) concentrations to palivizumab PK.

It has been suggested that 3 monthly doses of palivizumab may be sufficient to confer protection against RSV disease rather than the 5 monthly doses that were shown to be efficacious and supported registration of palivizumab (A. Solimano and E. Kwan, presented at the Pediatric Academic Societies, Boston, MA, 28 April to 1 May 2012). The abbreviated 3-month dosing is based on two assumptions. First, based on a half-life of 20 days, three doses of palivizumab will sustain concentrations over the entire RSV season, which is approximately 5 to 6 months in the United States (8). Second, with monthly dosing, the half-life of palivizumab increases over time (A. Solimano and E. Kwan, presented at the Pediatric Academic Societies, Boston, MA, 28 April to 1 May 2012). The final model was therefore used to simulate serum concentrations to compare differences in palivizumab exposure with abbreviated 3 monthly doses versus the recommended 5 monthly doses of 15 mg/kg.

MATERIALS AND METHODS

Twenty-two clinical studies contributed data to this analysis (Table 1). Seven studies were conducted in a total of 106 healthy adults (MI-CP007,

-CP017, -CP035, -CP080, -CP9401a, -CP9401b, and -CP9401c). Two studies were conducted in a total of 21 adults who had undergone bone marrow or stem cell transplants (MI-CP004 and -CP034). The adult PK data set was comprised of 116 subjects contributing a total of 1,661 palivizumab serum concentrations. The median (10th to 90th percentile) of the number of observations per patient was 13 (5 to 25.5).

The remaining 13 studies were conducted in infants and children comprising a total of 1,756 individuals: MI-CP005, -CP009, -CP011, -CP012, -CP013, -CP018, -CP026, -CP036, -CP045, -CP097, -CP116, -CP118, and -CP127. Ten of these studies ($n = 101$) were conducted in preterm infants less than or equal to 35 weeks of gestation at birth and 6 months of age or younger or children with CLD younger than or equal to 24 months (MI-CP005, -CP011, -CP012, -CP018, -CP036, -CP045, -CP097, -CP116, -CP118, and -CP127), all of which investigated multiple doses of palivizumab, except MI-CP045. Three of the pediatric studies were conducted in infants or children younger than 24 months who were hospitalized for RSV disease and received only 1 dose of palivizumab (MI-CP009, -CP013, and -CP026). Four of the pediatric studies involved intramuscular (i.m.) administration (MI-CP005, -CP009, -CP013, and -CP026), 8 involved intravenous (i.v.) administration, and 1 involved both (MI-CP045). The palivizumab pediatric PK data set was comprised of 1,684 patients contributing a total of 4,095 plasma palivizumab serum concentrations. The median (10th to 90th percentile) of the number of observations per patient was 2 (1 to 4).

Appropriate participant and institutional review board (IRB) approvals were received as part of each individual study.

Serum palivizumab immunoassay. Serum concentrations of palivizumab were measured by an enzyme-linked immunosorbent assay (ELISA) as previously described (26). Briefly, plates were coated with goat antipalivizumab antibody and serum was allowed to react with and bind to the fixed goat antipalivizumab antibody. The palivizumab-antipalivizumab complex was then treated with horseradish peroxidase-conjugated goat anti-human immunoglobulin G, and binding was detected by an enzymatic color reaction. The PK assay had an accuracy requirement for standards and controls of ±20% of nominal concentration and a precision requirement of ≤20% coefficient of variation (CV). The lower limit of quantitation of the PK method was 1.19 μg/ml.

Antipalivizumab antibody (ADA) was assessed by an ELISA developed and validated by MedImmune, LLC (Gaithersburg, MD), to detect ADA binding in serum. For this assay, plates were coated with palivizumab as the capture antigen. Serum samples were added to the plates and allowed to bind with palivizumab. The palivizumab-ADA complex was treated with horseradish peroxidase-conjugated palivizumab, and binding was detected by an enzymatic color reaction. A dilution series of a purified goat anti-idiotypic antipalivizumab antibody was included in each assay as a control. The method for measurement of ADA to palivizumab included a negative control and positive controls ranging from 0.24 to 1,000 ng/ml. Assay acceptance required the signal-to-background ratio (S:B) of the 1,000-ng/ml control to be ≥15. A postdose sample was reported positive for ADA to palivizumab if the measured signal, after subtraction of the predose sample's signal, was greater than or equal to twice the mean signal of the negative control (i.e., if the S:B was ≥2). The ELISA used to detect ADA is relatively drug intolerant and is subject to interference in the presence of palivizumab.

Data inclusion and exclusion criteria. Serum palivizumab concentration measurements that were missing or were below the analytical assay quantification limit or any values with unknown or missing associated observation times, dose times, dose amounts, or dosing intervals were excluded from the analysis. There were a total of 323 PK measurements that were below the limit of quantitation (BLQ), with 102 of these measurements occurring immediately following dosing. The 221 remaining BLQ records represented 3.6% of the data set. Given the small number of BLQ records, no methodology was implemented to account for the effect of BLQ values on parameter estimates. Individuals with no serum palivizumab concentration measurements were not included in the population PK data set.

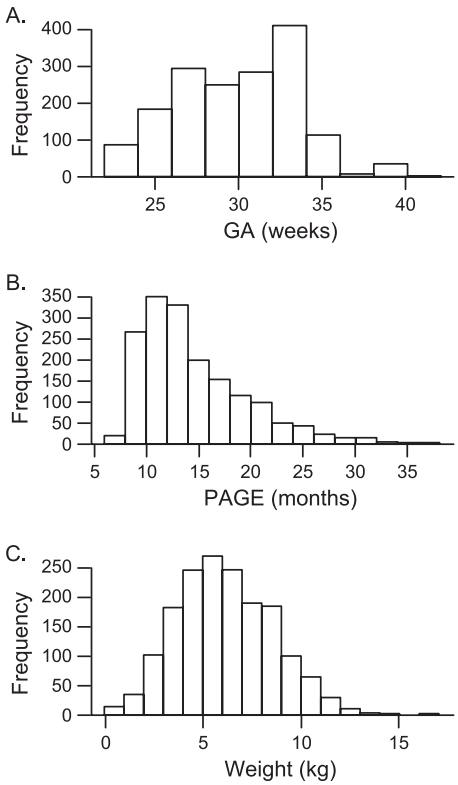

FIG 1 Distribution of demographic covariates at baseline: gestational age (GA) (A), GA + postnatal age (PAGE) (B), and weight (C).

Covariates used in the analyses. The covariates that were evaluated were sex, weight (kg), age, GA, GA + postnatal age (PAGE), ADA titer, disease state (CLD of prematurity, prematurity without CLD, and healthy term infant), and race (white, black, Hispanic, Asian, and other) (Fig. 1). ADA titers of ≥80 were combined into 1 category because of the limited numbers of patients with titers higher than 80 ($n = 17$); 63 patients had titers between 0 and 80, and 1,587 patients tested negative for ADA.

In the adult data set, there were 40 men and 76 women with a mean (range) age of 32.8 (19.3 to 58.9) years and a mean body weight of 72.5 (48.9 to 104.3) kg. The pediatric study data set consisted of 932 boys and 752 girls with a median (range) baseline body weight of 5.64 (0.92 to 16.3) kg, a median PAGE of 12.6 (6.89 to 34.7) months, and a median wGA of 30 (22 to 41). A majority of the pediatric patients were premature (62%), and 36% of patients had a diagnosis of CLD. The racial distribution of patients was 54% white, 20% black, 18% Hispanic, 2% Asian, and 6% other races.

Adjustments for covariates. Gestational age was imputed as 40 weeks for adults and full-term infants. Body weights of pediatric patients were recorded immediately before dosing with palivizumab. Because most pediatric patients were newborn, large relative changes in body weight during the 1-month interdose interval were observed. It was necessary to impute body weights between interdose intervals and at other times where serum concentration records were present without associated body weight information to avoid substantial effects on serum clearance (CL) or central volume of distribution (V_c). Body weight imputation for the pediatric population was based on PAGE (gestational age + AGE) using plots of body weight versus AGE or PAGE and used available body weight data in the calculation. PAGE was calculated as

$$\mathrm{PAGE} = \mathrm{AGE}\ (\mathrm{months}) + \frac{\mathrm{GA}\ (\mathrm{weeks})}{4.35\ (\mathrm{weeks/month})} \quad (1)$$

When body weight was missing for adult studies, the last nonmissing weight record was carried forward. For pediatric studies, missing body weight was imputed using the following equations, which are derived from the relationship between PAGE and patient body weight from RSV clinical trials.

When weight WT_i at $TIME_i$ was missing but with weight records available before and after $TIME_i$,

$$WT_t = WT_{t-1} + \frac{WT_{t+1} - WT_{t-1}}{TIME_{t+1} - TIME_{t-1}} \times (TIME_t - TIME_{t-1}) \quad (2)$$

When weight WT_i at $TIME_i$ was missing and all WT records were missing after $TIME_i$, WT_i was imputed according to the following algorithm.

If $PAGE_i < 13$, $WT_i = WT_{i-1} + 0.89\ (PAGE_i - PAGE_{i-1})$.

If $PAGE_i \geq 13$ and $PAGE_{i-1} \geq 13$, $WT_i = WT_{i-1} + 0.24\ (PAGE_i - PAGE_{i-1})$.

If $PAGE_i \geq 13$ but $PAGE_{i-1} < 13$, $WT_i = WT_{i-1} + 0.89\ (13 - PAGE_{i-1}) + 0.24\ (PAGE_i - 13)$.

Data analysis methods. Data were analyzed using nonlinear mixed-effect modeling (NONMEM) software, version VI, level 2.0 (Icon Development Solutions, Hanover, MD). The first-order conditional estimation with $\eta - \varepsilon$ interaction (FOCEI) was employed for all model runs. Model selection was guided by various goodness-of-fit criteria, including diagnostic scatter plots, plausibility of parameter estimates, and precision of parameter estimates, given the minimum objective function value and number of estimated parameters. Final model parameter estimates were reported with a measure of estimation uncertainty, including the asymptotic standard errors (obtained from the NONMEM $COVARIANCE step) and nonparametric bootstrap 95% confidence interval (CI).

Initial modeling was conducted using a 2-compartment model with first-order absorption to describe palivizumab absorption after i.m. injection. This model was parameterized in terms of clearance (CL), central volume of distribution (V_c), peripheral volume of distribution (V_p), intercompartmental clearance (Q), and absorption rate constant (k_a) (ADVAN4 TRANS4), with log-normal random effect distributions. The absolute bioavailability ($F1$) was estimated for i.m. palivizumab relative to i.v. administration. Residual variability was modeled using a proportional error model.

Initial modeling attempts to fit all adult and pediatric PK data simultaneously were largely unsuccessful due to the inability of the model to accurately characterize CL maturation parameters, which were dependent on initial estimates and produced large standard errors. This problem was likely due to the lack of data in children between 2 and 18 years of age. Therefore, the adult PK data were modeled first with the inclusion of allometrically scaled structural parameters to describe body size effects and the results from the adult analysis were used as prior information for fitting a population PK model to the pediatric data. This was implemented using the NONMEM $PRIOR subroutine, which is a restricted maximum-likelihood function for constraining parameter estimates based on prior knowledge.

Covariate model building. The full covariate modeling approach, which emphasized parameter estimation, rather than stepwise hypothesis testing, was used for this population PK analysis (7, 13, 16). The primary covariates of interest had been predefined for this analysis, based on mechanistic plausibility and prior knowledge. Body size was included as a covariate for CL, Q, V_c, and V_p. Additionally, the effects of PAGE, race, CLD of prematurity, and antibody titer were incorporated for CL. The effect of Hispanic race on V_c was also included in the full model based on results from population PK analysis of a monoclonal antibody of the same class.

Changes in physiologic parameters as a function of body size are both theoretically and empirically described as an allometric model (3, 5, 18).

$$TVP = \theta_{TVP} \times \left(\frac{WT_i\,(kg)}{70\,(kg)}\right)^{\theta allo} \quad (3)$$

The typical value of a model parameter (TVP) is described as a function of individual body weight (WT_i), normalized by a reference body weight of 70 kg, with a fixed allometric exponent (θ_{allo}) which is assigned a value of 0.75 for clearance processes and 1.0 for anatomical volumes. θ_{TVP} is an estimated parameter describing the typical PK parameter value for an individual with weight equal to the reference value.

Body weight changes alone do not adequately explain changes in drug disposition due to maturation of organ, tissues, enzyme, and transporter systems in neonates and infants (1, 3, 4). The effects of maturation on drug pharmacokinetics in young pediatric patients may be described by covariate models that consider age in addition to body size effects. Palivizumab clearance maturation was described via the following equation (1):

$$TVCL = \theta_{CL} \times \left(1 - \beta \times \exp^{-\left(\frac{PAGE - 40}{4.35}\right) \times \left(\frac{\ln(2)}{T_{CL}}\right)}\right) \quad (4)$$

where TVCL is the population typical value for CL, θ_{CL} is the allometrically scaled CL value, PAGE is in weeks, β is the fractional change in CL for a typical full-term (40-week PAGE) infant, and T_{CL} is the maturation half-life for CL.

Given the allometric weight-based model with maturation of CL with PAGE, the remaining predefined covariates were added to the population PK model to create a full covariate model. Population parameters including fixed-effect (covariate coefficients and structural model) and random-effect parameters were estimated. The full model is listed below.

$$\begin{aligned} CL_i = \theta_{CL} \times \left(\frac{WT_i(kg)}{70\,(kg)}\right)^{0.75} \times \left(1 - \beta \times \exp^{-\left(\frac{PAGE - 40}{4.35}\right) \times \left(\frac{\ln(2)}{T_{CL}}\right)}\right) \\ \times \theta 9^{RACE[AfricanAM]} \times \theta 10^{RACE[Hispanic]} \\ \times \theta 11^{RACE[Asian]} \times \theta 12^{RACE[Other]} \\ \times \theta 13^{CLD} \times \theta 17^{TITER[10]} \times \theta 18^{TITER[20]} \\ \times \theta 19^{TITER[40]} \times \theta 20^{TITER[\geq 80]} \times \exp^{\eta_{CL}} \end{aligned} \quad (5)$$

$$V_{C_i} = \theta_{VC} \times \left(\frac{WT_i\,(kg)}{70\,(kg)}\right)^{1.0} \times \theta 21^{RACE[Hispanic]} \quad (6)$$

$$V_{P_i} = \theta_{VP} \times \left(\frac{WT_i\,(kg)}{70\,(kg)}\right)^{1.0} \quad (7)$$

$$Q_i = \theta_Q \times \left(\frac{WT_i\,(kg)}{70\,(kg)}\right)^{0.75} \quad (8)$$

Inferences about clinical relevance of parameters were based on the resulting parameter estimates of the full model and measures of estimation precision (asymptotic standard errors, bootstrap 95% CI, or log-likelihood profile). Estimates of covariate effects were examined in the context of the magnitude of effect and precision of effect size.

Model evaluation. Simulations were performed using the final model parameter estimates to better understand the effect of GA and postnatal age on palivizumab serum concentrations in children of different postnatal ages and GAs receiving the recommended monthly dose of 15 mg/kg i.m. for a total of 5 doses. To describe population palivizumab exposures over the expected age and GA ranges, infants were divided into 3 different age ranges: 0 to 6 months, 7 to 12 months, and 13 to 24 months. Each age range was further categorized into GA ranges: 22 to 26 weeks, 27 to 31 weeks, 32 to 36 weeks, and 40 weeks. The final population PK model was used to simulate palivizumab concentrations in all 10 groups. Five hundred patients were simulated for 5 monthly doses using the final population PK model. The median and 95% prediction interval were plotted with observed data overlaid, stratified by study and dose. The precision of model parameters was investigated by performing a stratified nonparametric bootstrap procedure (9, 11, 12, 21). One thousand replicate data sets were generated by random sampling with replacement and were stratified by sex and age, using the individual as the sampling unit. Population parameters for each data set were subsequently estimated using NONMEM, resulting in a distribution of approximately 1,000 estimates for each population model parameter. Empirical 95% CIs were constructed by observing the 2.5th and 97.5th quantiles of the resulting pa-

rameter distributions for those bootstrap runs with successful convergence.

RESULTS

Adult population pharmacokinetic modeling results. A 2-compartment model was chosen as the adult population PK structural model. Body size effects on structural model parameters were described using allometric relationships, normalized to a patient weight of 70 kg (5, 20). The base model structural parameter estimates [% relative standard error] (CL = 198 [4.85%] ml/day, V_c = 2,200 [8.50%] ml, V_p = 2,410 [5.39%] ml, Q = 826 [10.1%] ml/day, $F1$ = 0.726 [7.40%], k_a = 0.373 [18.7%] day^{-1}) were relatively precise and were consistent with previously reported PK parameters for a monoclonal antibody without an antigen sink (10). Variance parameter estimates were also indicative of relatively large unexplained interindividual variability, with estimates of 43.4% coefficient of variation (CV%), 68.6 CV%, 41.5 CV%, and 65.3 CV% for CL, V_c, V_p, and Q, respectively.

Pediatric population pharmacokinetic modeling results. As suggested by the population analysis in adults, a 2-compartment linear model with first-order absorption was chosen as the base structural model. Body size effects on structural model parameters were described using allometric relationships, normalized to a patient body weight of 70 kg. The NONMEM $PRIOR subroutine was implemented to utilize the adult model results as informative priors for the predictive analysis.

The hyperparameters were described using a univariate normal distribution for fixed-effect parameters (e.g., THETA vector) and an inverse-Wishart distribution for the covariance matrix of interindividual random effects (e.g., OMEGA matrix). Equation 9 denotes the PK parameters corresponding to the prior value.

$$\Theta_{\text{prior}} = \begin{pmatrix} \text{CL} \\ V_c \\ V_p \\ Q \\ F1 \end{pmatrix} \quad \Omega_{\text{prior}} = \begin{pmatrix} \text{var}_{\text{CL}} & \text{COV}_{\text{CL}\ -\ V_c} \\ \text{COV}_{\text{CL}\ -\ V_c} & \text{var}_{V_c} \end{pmatrix} \tag{9}$$

Initial modeling attempts included the adult prior for k_a, but this prior was subsequently omitted due to suspected differences in absorption between adults and pediatric patients. Therefore, k_a was estimated solely from the pediatric data. Clearance maturation parameters (β, T_{CL}) were also estimated from the pediatric data. Attempts were made to estimate V_c maturation parameters, but the data did not support estimation of parameters for this model. The sparse nature of the pediatric PK data allowed for estimation of random effects for CL and V_c only.

All priors utilized in the NONMEM $PRIOR subroutine are shown in equation 10.

$$\Theta_{\text{prior}} \sim \left(\begin{pmatrix} 198 \\ 2,200 \\ 2,410 \\ 826 \\ 0.726 \end{pmatrix}, \begin{bmatrix} 92.2 & 0 & 0 & 0 & 0 \\ 0 & 34,969 & 0 & 0 & 0 \\ 0 & 0 & 6,900 & 0 & 0 \\ 0 & 0 & 0 & 6,956 & 0 \\ 0 & 0 & 0 & 0 & 0.00288 \end{bmatrix} \right) \tag{10}$$

$$\Omega_{\text{prior}} \sim \text{Wishart}^{-1}\left(\begin{bmatrix} 0.188 & 0.0160 \\ 0.0160 & 0.470 \end{bmatrix}, 10 \right)$$

Base model. The base model structural parameter estimates, normalized to a patient weight of 70 kg, were CL = 197 ml/day, V_c = 4,150 ml, V_p = 2,230 ml, Q = 874 ml/day, $F1$ = 0.686, k_a = 1.03 day^{-1}, fractional change in CL for a typical full-term (40-week PAGE) infant (β) = 0.438, and a maturation half-life of CL (T_{CL}) = 41.0 months. Variance parameter estimates were also indicative of relatively large interindividual variability, with estimates of 49.8 CV% and 61.6 CV% for CL and V_c, respectively. Random-effect parameters were not estimated for V_p and Q, given the sparse nature of the pediatric data and the inability to support estimation for these parameters.

Because highly correlated random-effect estimates were observed for CL and V_c, interindividual random-effect (ETA) shrinkage was calculated to understand the effects of the data structure on the empirical Bayes estimates. For the base model, ETA shrinkage was calculated to be 13.6% and 44.8% for CL and V_c random effects, respectively. Empirical Bayes individual random-effect estimates were not used to guide covariate selection.

Full model. The remaining predefined covariates were added to the population PK model to create a full covariate model in addition to the allometric weight-based model with maturation of CL with PAGE. The effect of CLD, race, ADA titer on CL, and Hispanic race on volume of distribution were implemented as categorical covariates. The full model resulted in a modest improvement in goodness-of-fit criteria compared with the base model. Similarly to the base model, there was considerable correlation between CL and V_c random effects.

Final model. The typical estimates for PK model parameters for the reference covariate effects (white, 70 kg, 40-week PAGE, ADA titer = 0) are presented in Table 2. Unexplained interindividual variability (CV%) was not substantially reduced for CL (48.7 CV%) and V_c (61.7 CV%) in the final model compared with the base model CL (49.8 CV%) and V_c (61.6 CV%) variance estimates. Although CL and V_c random effects were somewhat correlated (ρ = 0.62) in the final model, there was no issue with uniquely identifying random effects for these parameters. This is reasonable given the sparse nature of the pediatric PK data (mostly trough concentrations).

When maturational effects are accounted for, clearance estimates in the pediatric population were significantly reduced compared with adult values. The model parameter estimates scaled to a reference baseline body weight of 4.5 kg and 12.3-month PAGE (median values in study MI-CP018: 13.1-month PAGE and 4.5-kg body weight) are presented in Table 3. CL values in a typical patient between 7 and 18 months of PAGE were within approximately 10% of a typical child from the pivotal clinical study MI-CP018. CL ranged from 10.2 to 11.9 ml/day (1.17-fold change) as a function of PAGE over this range.

Patients with CLD of prematurity had a 20% increase in CL compared with premature and full-term infants. The effect estimate of 1.20 (95% CI, 1.13, 1.24) was precise, and the 95% CI did not include the null value of one. These data indicate that CLD of prematurity may influence clearance of palivizumab.

Clearance values were comparable among different races. All of the race effect parameters were small in magnitude and precisely estimated; the 95% CI of each estimate contained the null value of one (Table 2).

Patients with a positive ADA response had an elevated CL compared with those negative for ADA. At a titer of ≥80, there was a 20% increase in CL; the median CL value was 242 ml/day (versus 198 ml/day) with a relatively well-defined CI that did not overlap the reference value.

TABLE 2 Parameter estimates of final population pharmacokinetics model[a]

Parameter	Point estimate	% RSE	95% CI	IIV
CL × (WT/70)$^{0.75}$, ml/day	198	3.96	197, 198	48.7 (CV%)
θRACE = black	1.06	2.94	0.997, 1.14	
θRACE = Hispanic	1.05	3.52	0.985, 1.14	
θRACE = Asian	1.12	8.47	0.967, 1.32	
θRACE = other	1.10	4.65	0.999, 1.19	
θCLD	1.20	2.30	1.13, 1.24	
θtiter = 10	1.15	11.50	0.960, 1.45	
θtiter = 20	1.06	7.24	0.769, 1.25	
θtiter = 40	1.08	10.60	0.892, 1.35	
θtiter ≥ 80	1.21	8.35	1.07, 1.35	
V_c × (WT/70)$^{1.0}$, ml	4,090	3.20	3,508, 4,321	61.7 (CV%)
θRACE = Hispanic	1.06	6.69	0.921, 1.20	
V_p × (WT/70)$^{1.0}$, ml	2,230	3.83	1,694, 2,842	
Q × (WT/70)$^{0.75}$, ml/day	879	8.37	856, 967	
k_a, day^{-1}	1.01	13.10	0.691, 1.33	
$F1$	0.694	3.13	0.631, 0.733	
β	0.411	5.40	0.384, 0.452	
T_{CL}, mo	62.3	9.95	44.3, 94.3	
Residual variance				
σ^2_{prop}	0.0639	3.22	0.0618, 0.0900	
Residual variability proportional error CV	23.4 (CV%)			

[a] Estimates are for the typical patient (WT = 70 kg, RACE = white, no chronic lung disease of prematurity, antidrug antibody titer = 0). Abbreviations: % RSE, percent relative standard error of the parameter estimate; IIV, interindividual variability; WT, individual patient weight; CL, clearance; CV%, coefficient of variation; V_c, volume of distribution in the central compartment; V_p, volume of distribution in the peripheral compartment; Q, intercompartmental clearance; k_a, first-order absorption rate constant; $F1$, bioavailability; β, fractional decrease in CL for a typical patient with PAGE of 40 weeks; T_{CL}, CL maturation half-life; ω^2, interindividual variance; σ^2_{prop}, proportional residual variance.

TABLE 3 Parameter estimates from the final population PK model scaled to a reference of 4.5 kg and 12.3-month PAGE

Parameter	Point estimate (95% CI)
CL, ml/day	11.0 (10.3, 12.0)
V_c, ml	263 (226, 272)
V_p, ml	143 (109, 183)
Q, ml/day	112 (109, 123)
k_a, day^{-1}	1.01 (0.691, 1.33)
$F1$	0.694 (0.631, 0.733)

Model evaluation. The palivizumab population PK model evaluation results, which included the results of simulation and nonparametric bootstrap, revealed that the final model provided a reliable description of the data with good precision of structural model and variance parameter estimates. Simulation results, stratified by study and palivizumab dose, are shown in Fig. 2 (see also Fig. 4). The model closely describes observed palivizumab concentrations after monthly dosing at 15 mg/kg in study MI-CP018 (Fig. 2). The results of the simulation confirmed the appropriateness of the population fixed- and random-effect parameter values of the final model to adequately describe palivizumab concentrations in infants.

The stratified nonparametric bootstrap procedure resulted in 95% CIs for population PK parameter estimates, which are presented in the final model parameter table (Table 2). CIs were based on bootstrap estimates from 1,000 model runs that converged successfully, regardless of $COVARIANCE step success. Overall, typical structural model parameters, random variance terms, and covariate effects were estimated with good precision.

Population pharmacokinetic simulations. Specific simulations of expected concentration-time profiles (population typical value and 95% population prediction interval) were conducted with the final qualified model. Five hundred patients with the typical covariate values were simulated for comparison of 3 versus 5 consecutive monthly doses of palivizumab at 15 mg/kg. Five monthly palivizumab doses of 15 mg/kg provided sustained exposures over 150 days after the first dose compared with the abbreviated 3 monthly doses (Fig. 3).

Palivizumab PK profiles of 1,000 patients were simulated for each GA and age group (Fig. 4). The simulations show that GA has a minimal impact on palivizumab concentrations in all age groups. Palivizumab serum concentrations were similar across all 10 groups with a range of postnatal and gestational ages, indicating the appropriateness of body weight-based dosing (Fig. 5). Close agreement of predicted and observed concentrations and associated variability in concentrations was seen across all 10 groups. This further confirms the ability of the final population PK model to predict individual palivizumab concentrations for patients receiving palivizumab over a wide age and GA range.

DISCUSSION

The goals of this population PK analysis are to describe palivizumab PK in pediatric patients and to estimate the effects of covariates on the variability in palivizumab PK parameters. Initial modeling attempts were focused on fitting all of the adult and pediatric PK data simultaneously. This approach was largely unsuccessful, due to the inability of the model to accurately characterize CL maturation parameters. Using this methodology, maturation parameter estimates were dependent on initial estimates and produced large standard errors. This problem was likely due to the lack of data in children between 2 and 18 years of age. Therefore, an alternative modeling approach was applied where the adult PK data were first modeled with the inclusion of allometric models on structural parameters to describe body size effects. The results from the adult analysis were then used to fit a population PK model to the pediatric data, using the $PRIOR subroutine in NONMEM.

Modeling of palivizumab concentration data from adults alone indicated that palivizumab PK followed a 2-compartment model, with the PK parameter values of low CL of approximately 198 ml/day, limited central volume of distribution of 4.1 liters, and an intramuscular bioavailability of approximately 70% in healthy young adults. These values are typical of the pharmacokinetics of a monoclonal antibody without an antigen sink.

A 2-compartment linear model with first-order absorption described the structural PK model for palivizumab in adults and pediatric patients using allometry. Because allometric scaling alone did not adequately describe palivizumab disposition, a first-order function was used to describe the maturation of CL in children. As shown in Fig. 6, the clearance values of palivizumab in children are below those expected based on allometry alone. Studies by Anderson et al. (2, 3) show that changes in body weight

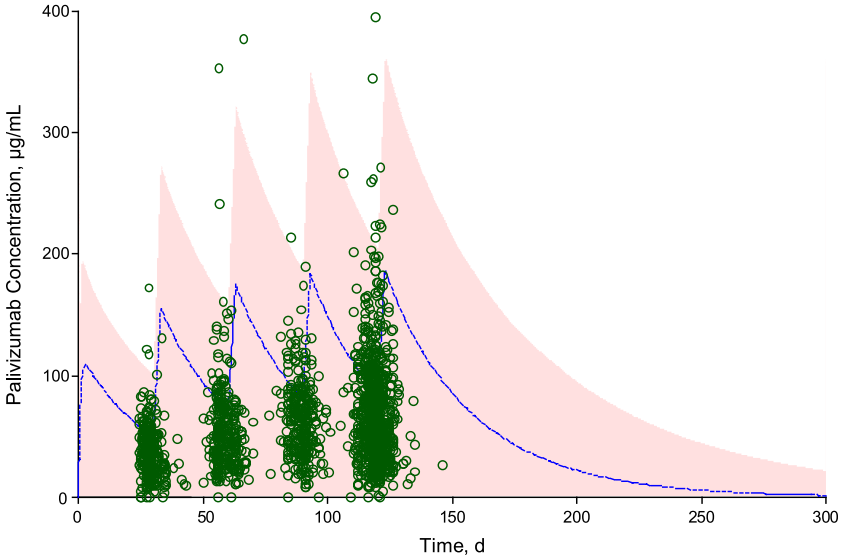

FIG 2 Simulated concentration-time profiles from study MI-CP018 at 15 mg/kg. Observed palivizumab concentrations (open circles) are plotted with the population median concentration (dashed line) and the associated 95% prediction interval (shaded area).

alone do not adequately explain the changes in CL and volume of distribution in pediatric patients; maturational effects must also be considered as different organ/tissue/enzyme/transporter systems evolve and mature. Therefore, age and body weight were evaluated to characterize palivizumab PK in the infant population before covariate analysis. There are 2 age descriptors for this population, GA and postnatal age. Because drug elimination mechanisms mature throughout gestation and after birth (5), PAGE, the sum of GA and postnatal age, is suitable and accounts for changes in clearance and central volume of distribution in infants. For palivizumab, the relationship between PAGE and CL was observed, but the data did not support estimation of V_c maturation parameters.

Palivizumab absorption was faster in pediatric patients (k_a = 1.01/day) than in healthy adults (k_a = 0.373/day), whereas the bioavailability values of palivizumab were similar (about 70%) in adults and children. It is not known whether this difference represents actual changes in palivizumab absorption with age or an artifact of study design (dense PK sampling in adults, sparse PK sampling in children). Therefore, k_a was estimated from the pediatric data with no prior value given for adults.

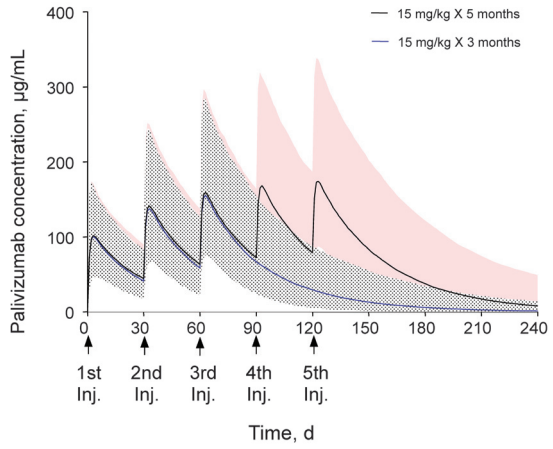

FIG 3 Simulated concentration-time profiles from the abbreviated 3 monthly 15-mg/kg doses of palivizumab compared with 5 monthly doses. Solid lines are the median predicted concentrations; shaded areas are the 95% prediction intervals.

The covariate modeling approach, which emphasized parameter estimation rather than stepwise hypothesis testing, was used for this population PK analysis to avoid issues associated with the likelihood ratio test in mixed-effect models, including correlation or colinearity of predictors, multiple comparisons, and artificial parameter precisions (7, 16). Results of the covariate analysis identified a 20% lower CL in infants without CLD than in infants with CLD. However, there was substantial overlap in the range of individual CL values from infants with and without CLD. The mechanism for the slightly greater clearance in infants with CLD is not clear. The slightly lower CL in infants without CLD is expected to translate into slightly higher concentrations compared with infants with CLD, but these slightly increased concentrations in CLD infants are expected to be inconsequential compared with the much larger unexplained interindividual variability of 48.8% in CL and residual variability in concentrations.

Patients with a positive ADA response had an elevated clearance compared with those negative for ADA. This effect was not significant at low ADA titer values of $<$80. At a titer of $\geq$80, there was an approximately 20% increase in CL. The effect estimate of 1.21 (95% CI, 1.07, 1.35) did not include the null value of 1, suggesting that patients with titers of $\geq$80 would have increased palivizumab CL. The total number of patients with ADA titer values of $\geq$80 was small (17 of 1,667). There was a $<$50% probability that a patient with a titer of $\geq$80 would have a CL value with a greater than 25% increase compared to the typical patient (Fig. 7). For titer values of $\geq$80, the median CL value was 242 ml/day (versus 198 ml/day) with a relatively well-defined CI that did not overlap the reference value. None of the covariates examined in this analysis explained a significant portion of variability in palivizumab PK.

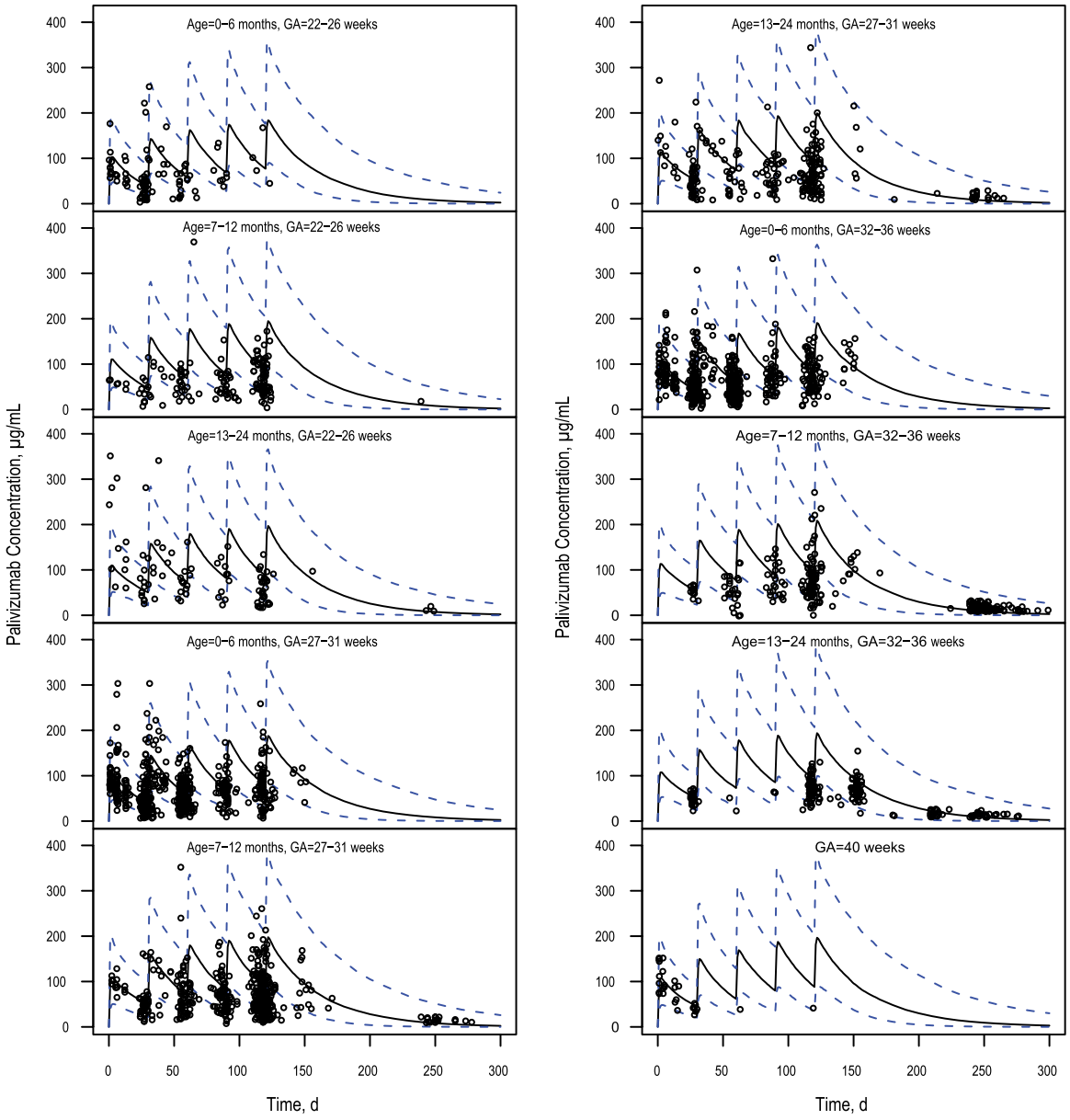

FIG 4 Simulated and observed concentration-time profiles for 15-mg/kg dose of palivizumab, stratified by age and gestational age (GA). Solid black lines are the simulated medians, blue dashed lines are the 95% prediction intervals, closed circles are predicted values, and open circles are the observed values.

The ability of the final model to predict palivizumab concentrations in groups varying in age and GA was tested by comparing the predicted concentrations with observed concentrations and variability. Close agreement of the predicted and observed concentrations and associated variability was seen across all groups examined, suggesting that palivizumab PK did not differ between healthy term and preterm infants and indicating that GA has a minimal effect on palivizumab concentrations in all age groups. Simulations performed across 3 age groups, spanning postnatal ages of 0 to 24 months and GAs of 22 to 40 weeks, indicate that median trough concentrations among the 3 age groups are essentially similar. Because palivizumab concentrations and concentration-time profiles were similar across different postnatal age (0 to 24 months) and GA (22 to 40 weeks) groups encompassing the entire palivizumab-treated population (Fig. 2), the use of the body weight-corrected dose of 15 mg/kg for this entire population is supported. Consideration of GA is only helpful for modeling purposes to identify PK parameters accurately, especially at low postnatal ages (0 to 6 months).

Although efficacy for the prevention of RSV hospitalization in children with prematurity or CLD was defined in a clinical trial with a regimen of 5 monthly doses of 15 mg/kg palivizumab (22), 3 doses have been suggested as an alternative dosing regimen based on the assumption of increasing half-life of palivizumab with monthly dosing. Simulations conducted using the final palivizumab pediatric population PK model to compare palivizumab exposures from abbreviated 15-mg/kg monthly dosing for 3 months with the label-indicated regimen of 5 monthly 15-mg/kg

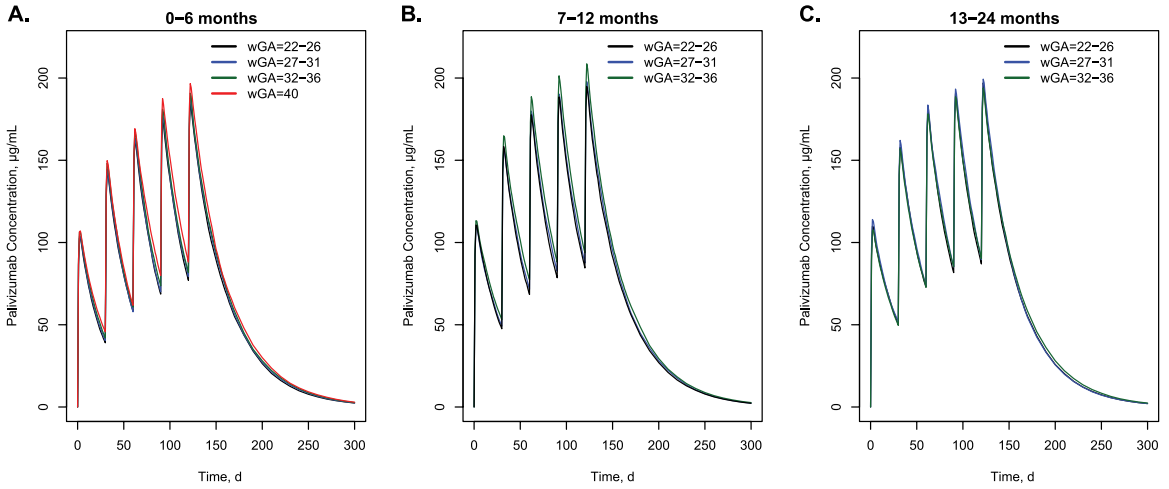

FIG 5 Group median concentration-time profiles of palivizumab at 15 mg/kg stratified by GA + postnatal age (PAGE) and postnatal age cohorts, 0 to 6 months (A), 7 to 12 months (B), and 13 to 24 months (C).

doses clearly show that palivizumab follows linear PK typical of an IgG1 monoclonal antibody with no change in half-life with time, and more importantly, the regimen of 15 mg/kg monthly for 5 months intended to cover the entire RSV season provides increased exposure with prolonged palivizumab concentrations compared with concentrations at month 5 after 3 monthly palivizumab doses. These analyses suggest that palivizumab concentrations from the abbreviated 3 monthly doses would yield lower exposures than would the regimen of 5 monthly 15-mg/kg doses, which has been demonstrated to be efficacious in preventing RSV hospitalizations during the course of a typical RSV season.

Conclusions. Palivizumab PK and variability in serum concentrations are typical of those of an IgG1 monoclonal antibody. The population PK of palivizumab in adults and pediatric patients is described best by a 2-compartment linear model with first-order absorption to describe i.m. absorption. Palivizumab clearance in children is best predicted by considering maturation of CL in children and body weight. There is little difference in palivizumab PK in healthy term and premature infants. GA has a minimal effect on palivizumab concentrations.

Covariate modeling did not identify covariates that could explain the 49% interindividual variability in CL or the 25% residual variability in palivizumab concentrations seen in the clinical studies after body weight-based dosing. Palivizumab clearance is slightly higher in pediatric patients with CLD and in patients who develop ADA titers of ≥80. None of the covariates explain interindividual variability in palivizumab PK to any meaningful extent. This means that unexplained variability in serum concentrations is not related to any demographic factor, making it difficult to predict serum concentrations *a priori* on an individual basis. The similar mean concentrations seen across a range of GAs and postnatal ages in children confirm the adequacy of body weight-based dosing of palivizumab in pediatric patients. The body weight-corrected dose of 15 mg/kg yields comparable therapeutic concentrations for all pediatric patients with varied demographic characteristics in the palivizumab-treated population.

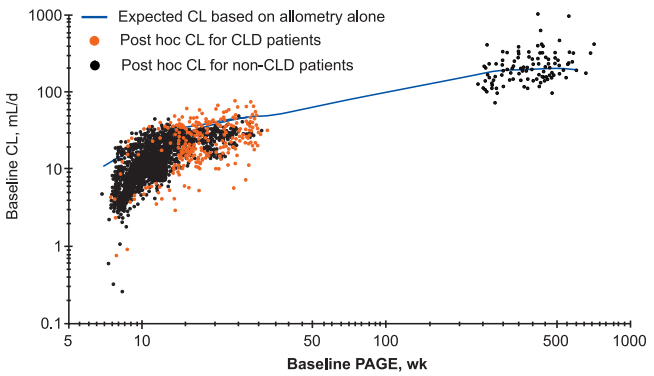

FIG 6 Comparison of *post hoc* clearance values in children compared with clearance values expected based on allometry alone.

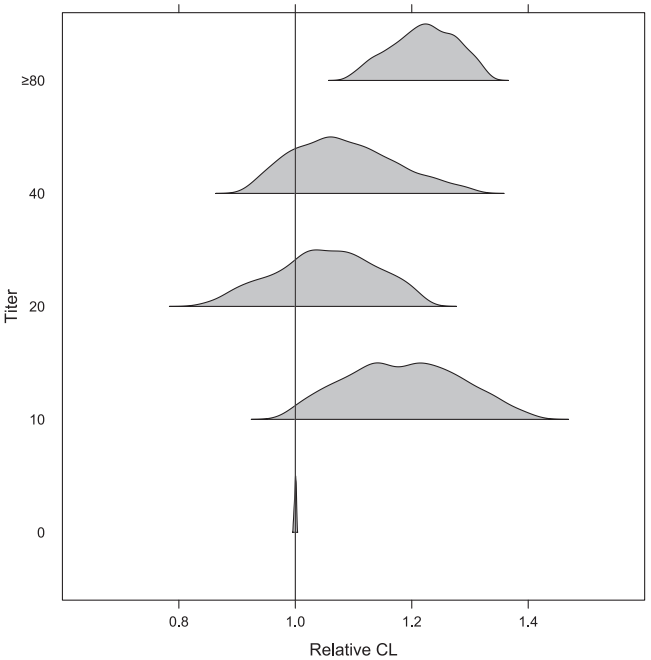

FIG 7 Covariate effects of ADA titer on clearance. Typical clearance is presented for the reference patient (70 kg, white, titer = 0, no CLD).

Simulations demonstrate that the palivizumab label-indicated dosing of 15 mg/kg administered monthly for a total of 5 doses provides increased and prolonged palivizumab exposure over the entire RSV season compared with abbreviated dosing regimens of 3 monthly doses. At this time, the regimen of 5 monthly doses, which showed efficacy in two randomized clinical trials, remains the only dosing regimen adequately studied in humans. These results, in conjunction with the marked interpatient variability in serum concentrations, highlight the risk of suboptimal dosing with the off-label 3-monthly dosing regimen.

ACKNOWLEDGMENTS

We thank Marc Gastonguay from Metrum Research Group and Tracy E. Bunting-Early, John E. Fincke, and Gerard P. Johnson of Complete Healthcare Communications Inc. (Chadds Ford, PA) for editorial assistance funded by MedImmune.

In regard to potential conflicts of interest, this study was sponsored by MedImmune, LLC. G. J. Robbie, G. Losonsky, and L. K. Roskos are employees of MedImmune. L. Zhao was an employee of MedImmune at the time of the analysis. MedImmune was involved in the study design; collection, analysis, and interpretation of data; the writing of this report; and the decision to submit this paper for publication.

REFERENCES

1. **Anderson BJ, Allegaert K, Holford NH.** 2006. Population clinical pharmacology of children: modelling covariate effects. Eur. J. Pediatr. **165**: 819–829.
2. **Anderson BJ, Allegaert K, Van den Anker JN, Cossey V, Holford NH.** 2007. Vancomycin pharmacokinetics in preterm neonates and the prediction of adult clearance. Br. J. Clin. Pharmacol. **63**:75–84.
3. **Anderson BJ, Holford NH.** 2008. Mechanism-based concepts of size and maturity in pharmacokinetics. Annu. Rev. Pharmacol. Toxicol. **48**:303–332.
4. **Anderson BJ, Holford NH.** 2009. Mechanistic basis of using body size and maturation to predict clearance in humans. Drug Metab. Pharmacokinet. **24**:25–36.
5. **Anderson BJ, Woollard GA, Holford NH.** 2000. A model for size and age changes in the pharmacokinetics of paracetamol in neonates, infants and children. Br. J. Clin. Pharmacol. **50**:125–134.
6. **Brandt CD, et al.** 1973. Epidemiology of respiratory syncytial virus infection in Washington, D.C. 3. Composite analysis of eleven consecutive yearly epidemics. Am. J. Epidemiol. **98**:355–364.
7. **Burnham KP, Anderson DR.** 2002. Model selection and multimodel inference: a practical information-theoretic approach. Springer-Verlag, New York, NY.
8. **Centers for Disease Control and Prevention.** 2011. Respiratory syncytial virus-United States, July 2007–June 2011. MMWR Morbid. Mortal. Wkly. Rep. **60**:1203–1206.
9. **Chiou WL.** 1989. The phenomenon and rationale of marked dependence of drug concentration on blood sampling site. Implications in pharmacokinetics, pharmacodynamics, toxicology and therapeutics (part I). Clin. Pharmacokinet. **17**:175–199.
10. **Dirks NL, Meibohm B.** 2010. Population pharmacokinetics of therapeutic monoclonal antibodies. Clin. Pharmacokinet. **49**:633–659.
11. **Ette EI.** 1997. Stability and performance of a population pharmacokinetic model. J. Clin. Pharmacol. **37**:486–495.
12. **Ette EI, Onyiah LC.** 2002. Estimating inestimable standard errors in population pharmacokinetic studies: the bootstrap with Winsorization. Eur. J. Drug Metab. Pharmacokinet. **27**:213–224.
13. **Gastonguay M.** 2011. Full covariate models as an alternative to methods relying on statistical significance for inferences about covariate effects: a review of methodology and 42 case studies, abstr 2229. Abstr. Annu. Meet. Popul. Approach Group Eur. http://www.page-meeting.org/?abstr=2229.
14. **Glezen P, Denny FW.** 1973. Epidemiology of acute lower respiratory disease in children. N. Engl. J. Med. **288**:498–505.
15. **Hall CB, Kopelman AE, Douglas RG, Jr, Geiman JM, Meagher MP.** 1979. Neonatal respiratory syncytial virus infection. N. Engl. J. Med. **300**: 393–396.
16. **Harrell F.** 2001. Regression modeling strategies with applications to linear models, logistic regression, and survival analysis. Springer Verlag, New York, NY.
17. **IMpact Study Group-RSV.** 1998. Palivizumab, a humanized respiratory syncytial virus monoclonal antibody, reduces hospitalization from respiratory syncytial virus infection in high-risk infants. Pediatrics **102**(3 Pt 1):531–537.
18. **Jonsson EN, Karlsson MO.** 1998. Automated covariate model building within NONMEM. Pharm. Res. **15**:1463–1468.
19. **MedImmune.** 2012. Synagis. Palivizumab. Package insert. MedImmune, Gaithersburg, MD.
20. **Meibohm B, Laer S, Panetta JC, Barrett JS.** 2005. Population pharmacokinetic studies in pediatrics: issues in design and analysis. AAPS J. **7**:E475–E487.
21. **Parke J, Holford NH, Charles BG.** 1999. A procedure for generating bootstrap samples for the validation of nonlinear mixed-effects population models. Comput. Methods Programs Biomed. **59**:19–29.
22. **Parnes C, et al.** 2003. Palivizumab prophylaxis of respiratory syncytial virus disease in 2000–2001: results from The Palivizumab Outcomes Registry. Pediatr. Pulmonol. **35**:484–489.
23. **Saez-Llorens X, et al.** 2004. Safety and pharmacokinetics of palivizumab therapy in children hospitalized with respiratory syncytial virus infection. Pediatr. Infect. Dis. J. **23**:707–712.
24. **Shay DK, et al.** 1999. Bronchiolitis-associated hospitalizations among US children, 1980–1996. JAMA **282**:1440–1446.
25. **Shay DK, Holman RC, Roosevelt GE, Clarke MJ, Anderson LJ.** 2001. Bronchiolitis-associated mortality and estimates of respiratory syncytial virus-associated deaths among US children, 1979–1997. J. Infect. Dis. **183**:16–22.
26. **Subramanian KN, et al.** 1998. Safety, tolerance and pharmacokinetics of a humanized monoclonal antibody to respiratory syncytial virus in premature infants and infants with bronchopulmonary dysplasia. MEDI-493 Study Group. Pediatr. Infect. Dis. J. **17**:110–115.
27. **Thompson WW, et al.** 2003. Mortality associated with influenza and respiratory syncytial virus in the United States. JAMA **289**:179–186.